Stability analysis and μ-synthesis control of brake systems

S. Lignon*, J-J. Sinou, L. Jézéquel

Laboratoire de Tribologie et Dynamique des Systèmes, Equipe Dynamique des Structures et des Systèmes, Ecole Centrale de Lyon, Batiment E6, 36 Avenue Guy de Collongue, 69134 Ecully Cedex, France

Abstract

The concept of friction-induced brake vibrations, commonly known as judder, is investigated. Judder vibration is based on the class of geometrically induced or kinematic constraint instability. After presenting the modal coupling mechanism and the associated dynamic model, a stability analysis as well as a sensitivity analysis have been conducted in order to identify physical parameters for a brake design avoiding friction-induced judder instability.

Next, in order to reduce the size of the instability regions in relation to possible system parameter combinations, robust stability via μ-synthesis is applied. By comparing the unstable regions between the initial and controlled brake system, some general indications emerge and it appears that robust stability via μ-synthesis has some effect on the instability of the brake system.

© 2006 Elsevier Ltd. All rights reserved.

1. Introduction

Friction-induced vibration and instability are complicated phenomena that have been studied in detail by many researchers [1–23]. However, they are still a major concern in a wide range of mechanical systems due to the difficulty in resolving the problem. This is especially the case for brake systems, where friction-induced vibration due to coupling modes can cause severe damage or/and noise. So the prevention and prediction of unstable vibrations are actually very complex and important problems for the vehicle brake industry. In order to avoid these problems, the effects of some specific system parameters (typically mass, stiffness, damping, etc.) need to be studied in order to detect the stable and unstable zones of the mechanical system subject to friction-induced instability. Though many studies have been conducted and some of them have been successfully applied to particular brake systems and running conditions, it can be very difficult to find suitable values of the system parameters in order to obtain stable brake systems for all operating conditions. In these cases, the engineer therefore needs to find suitable devices to control instability in the brake system.

In recent decades, friction-induced vibration has received considerable attention from a number of researchers: Ibrahim [1,2], Bowden and Tabor [3], Rabinowitz [4], Armstrong-Hélouvry [5], and Oden and Martins [6]. Their investigations were conducted in order to find different mechanisms of friction-induced

*Corresponding author. Tel.: +33 4 72 18 64 64; fax: +33 4 72 18 91 44.

E-mail address: sylvain.lignon@ec-lyon.fr (S. Lignon).

Nomenclature		x	scalar
		$\mathbf{x}$	vector
$\mathbf{C}$	damping matrix	$\dot{\mathbf{x}}$	vector of velocity
$\mathbf{G}$	controller	$\ddot{\mathbf{x}}$	vector of acceleration
$\mathbf{K}$	stiffness matrix	$\varDelta_{\mathrm{set}}$	structured uncertainties set
$\mathbf{M}$	mass matrix	λ	eigenvalue of the nominal system
N	normal load	$\tilde{\lambda}$	eigenvalue of the controlled system
$\mathbf{P}$	initial system	μ_f	brake friction coefficient
T	tangential load	μ	structured singular value

system instability. This type of analysis was then introduced in the context of brake noise to predict the dynamic behaviour of brake systems and to prevent instability (Ouyang et al. [12], North [7,8], Kinkaid et al. [10], etc.).

In order to find the most suitable mechanism to describe friction-induced vibration in brake systems, these different mechanisms have to be examined. They fall into four classes: stick-slip, variable dynamic friction coefficient, sprag-slip [22] and geometric coupling of degrees of freedom [9,15–21]. The sprag-slip action was described by Spurr [22] and does not depend on a friction coefficient varying with the relative rotation speed of the brake disc. Next, a number of investigations have been developed by considering kinematic constraint or geometric instability. This mechanism involves the coupling of the different degrees of freedom. It can be seen as an extension of the idea of the sprag-slip model [22]. Earles et al. [15,16,18,20] and North [7,8] conducted extensive studies of kinematical constrained instability models. They demonstrated that instability may occur even if the friction coefficient is constant.

In this study, a modal coupling mechanism involving two system modes coupled together due to the friction interface will be considered. This instability may be defined as a geometrical coupling where two system modes move closer in frequency as the friction coefficient increases.

In this study, the application of robust control via μ-synthesis for a brake system is tested in order to avoid instability or in order to reduce the instability regions. In the first section, some basic concepts of μ-synthesis will be introduced. In the second section, the modal coupling mechanism used in this study will be briefly presented and the application of μ-synthesis for judder instability will be investigated. Next, a stability analysis and some interesting studies of possible system parameter combinations for the initial and controlled brake systems will be undertaken in order to examine the varying effects of robust control analysis on the size of the instability regions. This sensitivity analysis will be conducted in order to find the physical parameters for a brake design which avoid friction-induced instability in the case of controlled and uncontrolled brake systems. Finally, some natural extensions and possible applications of this methodology will be briefly described in the conclusions.

2. μ-synthesis

2.1. Introduction

The robustness of a system $\mathbf{P}$ with uncertainties represented by a set $\mathbf{\Delta}_{\mathrm{set}}$ of block-diagonal matrices is studied with the non-singularity of the matrix $\mathbf{I} - \mathbf{P}\mathbf{\Delta}$ (where $\mathbf{I}$ is the identity matrix), for $\mathbf{\Delta} \in \mathbf{\Delta}_{\mathrm{set}}$. In order to treat this problem, the structured singular value μ is introduced; this parameter μ will be defined below.

This theory was introduced by Doyle [24] in 1982 and has become a standard tool in the robustness analysis of linear systems. It directly considers the problem of robust stability for a known plant subject to a block-diagonal structured uncertainty connected in feedback. The utility of μ lies in the fact that essentially any block diagram interconnection of systems and uncertainties may easily be rearranged into this standard form, i.e. where the uncertainty structure is block-diagonal.

2.2. Structured singular value

This section defines the structured singular value $\mu(\cdot)$. We consider matrices $\mathbf{P} \in \mathbf{R}^{n \times n}$ and introduce a structure $\mathbf{\Delta}_{\text{set}}$ to define $\mu(\mathbf{P})$. This structure $\mathbf{\Delta}_{\text{set}}$ is a prescribed set of block-diagonal matrices and may be defined differently for each problem depending on the uncertainty of the problem.

By definition, $\mu(\mathbf{P})$ is defined for $\mathbf{P} \in \mathbf{C}^{n \times n}$ by

$$\mu(\mathbf{P}) = \frac{1}{\min\{\bar{\sigma}(\mathbf{\Delta}) : \mathbf{\Delta} \in \mathbf{\Delta}_{\text{set}}, \det(\mathbf{I} - \mathbf{P}\mathbf{\Delta}) = 0\}} \tag{1}$$

unless no $\mathbf{\Delta} \in \mathbf{\Delta}_{\text{set}}$ makes $\mathbf{I} - \mathbf{P}\mathbf{\Delta}$ singular, in which case $\mu(\mathbf{P}) = 0$. $\bar{\sigma}(\mathbf{\Delta})$ corresponds to the maximum singular value of the matrix $\mathbf{\Delta}$.

μ is then a function of two variables: the complex matrix $\mathbf{P}$ and the structure $\mathbf{\Delta}_{\text{set}}$.

Considering the loop shown in Fig. 1, $\mu(\mathbf{P})$ can be interpreted as a measure of the smallest uncertainty (represented by the matrix $\mathbf{\Delta}$) that causes instability of the constant matrix feedback loop. The norm of this destabilizing $\mathbf{\Delta}$ is exactly $1/\mu(\mathbf{P})$. It means that the weaker $\mu(\mathbf{P})$ is, the more robust the system.

Details concerning the calculation of the structured singular value are given in Packard and Doyle [25].

2.3. μ-synthesis

The definition of μ allows an extension of the stability analysis of systems by considering the system illustrated in Fig. 2. This system is composed of three blocks $\mathbf{\Delta}$, $\mathbf{P}$ and $\mathbf{G}$ that define the perturbation matrix, the initial system which should be controlled, and the controller, respectively.

The input/output couples are (u_0, Y_0), (u_1, Y_1) and (u_2, Y_2) which define respectively the perturbation variables associated with the perturbation matrix $\mathbf{\Delta}$, the measurable output (with the input control u_1) and the performance variables where u_2 includes the commands and the excitation and Y_2 represents the errors and the results.
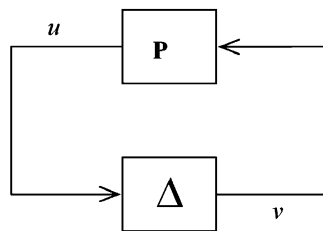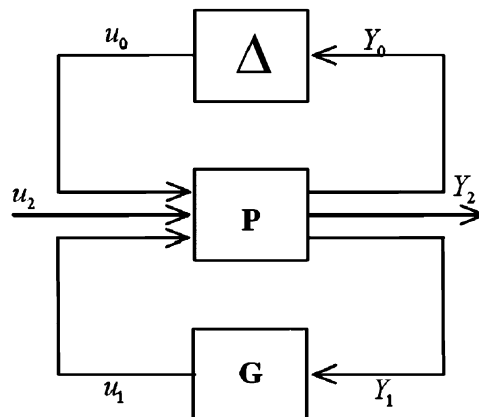

Fig. 1. $\mathbf{P} - \mathbf{\Delta}$ feedback connection.

Fig. 2. General structure of the problem.

Then, μ-synthesis consists of determining the controller **G** allowing the stability of the system in the presence of the uncertainty Δ. The resolution is conducted by applying successive iterations. As the controller is often denoted by **K** (notation already used here for the stiffness matrix), this resolution is called the D–K iterations. These iterations are repeated unless $\mu < 1$. If $\mu < 1$, the robust stability of the system is assured for the given uncertainties. The theory of μ-synthesis is developed in Packard et al. [26], Venini [27], Balas et al. [28] and Markerink et al. [29]. Some applications can be found in Lanzon [30], Wu and Lin [31].

3. Brake systems

In order to demonstrate the suitability of μ-synthesis to brake systems and in order to link the effect of specific parameter variation with stability of the design features, a parameter model including friction forces at the rubbing surface and mechanisms for friction-induced system instability is established and the equations of motion are determined.

The problem considered in this study deals with a modal coupling mechanism [11,12] that results from the coupling of two system modes due to the friction interface. The first mode corresponds to the suspension mode of the front axle assembly and the second mode corresponds to the normal mode of the brake piston elements. This phenomenological model was established through experimental investigations [32] and the friction-induced vibration was observed in the 50–100 Hz range without variation of the brake friction coefficient. The fact that instability may occur even if the coefficient of friction is constant is a very common phenomenon that has been observed by many researchers [9,11,15–21].

In the following sections, two analytical models (the initial and controlled systems) will first be presented. Second, a stability analysis for each system will be undertaken and the initial and controlled systems will be compared in order to demonstrate the suitability of robust control for brake systems.

3.1. Initial system

The initial system studied here is modelled as a three-degrees-of-freedom system, as illustrated in Fig. 3(A): translational and normal displacement in the y-direction of the mass m_2 defined by $Y_2(t)$ and $X_2(t)$, respectively, and the translational displacement in the x-direction of the mass m_1 defined by $X_1(t)$. As previously explained, each mode is linked to a single vibration mode of the brake system: (k_1, m_1) and (k_2, m_2) define the dynamic of the brake piston elements and the dynamic of the suspension mode of the front axle assembly, respectively. The modal coupling mechanism involves the two modes coupled together due to the
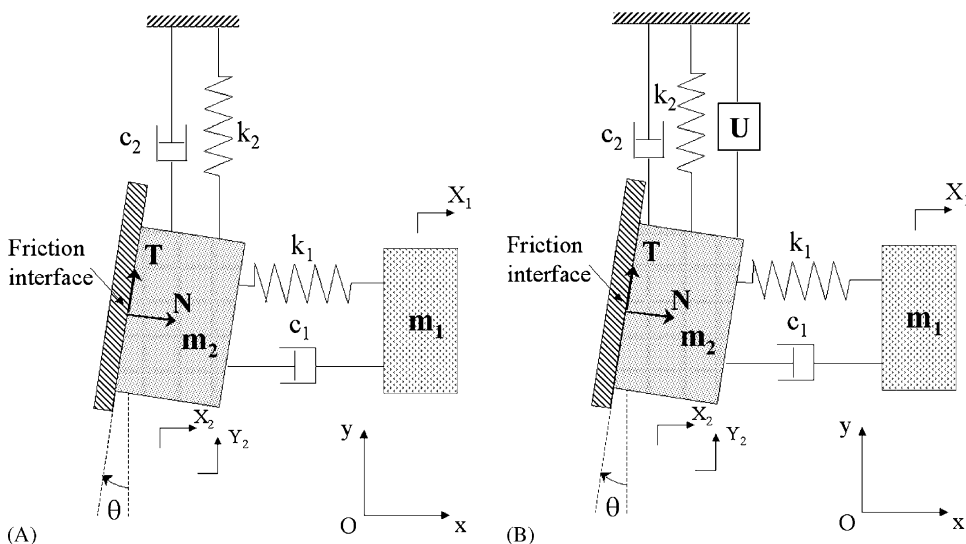

Fig. 3. Braking model (A) initial system (B) controlled system.

friction interface. This mechanism may induce a classic flutter instability where two solutions for the dynamic behaviour of the mechanical system exist. The first solution is an unstable equilibrium whereas the second is a periodic solution. Then, any perturbation of the equilibrium point implies self-excited vibrations.

In order to simulate the modal coupling mechanism due to the friction interface, this friction interface slopes with an angle θ. This assumption may be seen as a geometric coupling with the braking system. This slope couples the normal and tangential degrees-of-freedom induced by the brake friction coefficient only.

By considering this system composed of two masses m_1 and m_2 interconnected by stiffnesses k_1 and k_2 (Fig. 3), the dynamic equilibrium around its static equilibrium position is expressed by the following system of equations:

$$
\begin{aligned}
& m_1 \ddot{X}_1 + c_1(\dot{X}_1 - \dot{X}_2) + k_1(X_1 - X_2) = 0, \\
& m_2 \ddot{Y}_2 + c_2 \dot{Y}_2 + k_2 Y_2 = -N \sin \theta + T \cos \theta, \\
& m_2 \ddot{X}_2 + c_1(\dot{X}_2 - \dot{X}_1) + k_1(X_2 - X_1) = N \cos \theta + T \sin \theta.
\end{aligned}
\tag{2}
$$

By applying the hypothesis of maintained contact between the mass m_2 and the moving belt, the geometric constraint imposes

$$
X_2 = Y_2 \tan \theta.
\tag{3}
$$

By eliminating X_2 in Eq. (3) and considering Coulomb's friction law $T = \mu_f N$, the 2-degrees-of-freedom system has the form

$$
\mathbf{M}\ddot{\mathbf{x}} + \mathbf{C}\dot{\mathbf{x}} + \mathbf{K}\mathbf{x} = \mathbf{0},
\tag{4}
$$

where $\mathbf{x} = \{ X_1 \quad Y_2 \}^{\mathrm{T}}$. $\ddot{\mathbf{x}}$, $\dot{\mathbf{x}}$ and $\mathbf{x}$ are the acceleration, velocity and displacement response two-dimensional vectors of the degrees-of-freedom, respectively. The mass matrix $\mathbf{M}$, the damping matrix $\mathbf{C}$ and the stiffness matrix $\mathbf{K}$ of the system are given by

$$
\mathbf{M} = \begin{bmatrix} m_1 & 0 \\ 0 & m_2(\tan^2 \theta + 1) \end{bmatrix},
\tag{5}
$$

$$
\mathbf{C} = \begin{bmatrix} c_1 & -c_1 \tan \theta \\ c_1(-\tan \theta + \mu_f) & c_1(\tan^2 \theta - \mu_f \tan \theta) + c_2(1 + \mu_f \tan \theta) \end{bmatrix},
\tag{6}
$$

$$
\mathbf{K} = \begin{bmatrix} k_1 & -k_1 \tan \theta \\ k_1(-\tan \theta + \mu_f) & k_2(1 + \mu_f \tan \theta) + k_1(\tan^2 \theta - \mu_f \tan \theta) \end{bmatrix}.
\tag{7}
$$

Finally, the dynamic system may be rewritten in state variables:

$$
\dot{\mathbf{z}} = \mathbf{A}\mathbf{z},
\tag{8}
$$

where

$$
\mathbf{z} = \begin{bmatrix} \mathbf{x} \\ \dot{\mathbf{x}} \end{bmatrix}
\tag{9}
$$

and

$$
\mathbf{A} = \begin{bmatrix} \mathbf{0} & \mathbf{I} \\ -\mathbf{M}^{-1}\mathbf{K} & -\mathbf{M}^{-1}\mathbf{C} \end{bmatrix}.
\tag{10}
$$

3.2. Controlled system by applying μ-synthesis

μ-synthesis is applied to the brake system by assuming that the friction coefficient μ_f is uncertain. This uncertainty corresponds to possible variations of the friction with time. This controlled system is illustrated in Fig. 3(B): the controller U is placed in parallel with the suspension.

3.2.1. Definition of the controlled system

By considering Section 2 and Eqs. (15–17) of the initial brake system, the nominal system is represented by

$$\dot{\mathbf{z}} = \mathbf{A}\mathbf{z} + \mathbf{B}_1\mathbf{u}_1,$$
$$\mathbf{y}_1 = \mathbf{C}_1\mathbf{z} + \mathbf{D}_{11}\mathbf{u}_1, \tag{11}$$

where

$$\mathbf{B}_1 = \begin{bmatrix} 0 \\ 0 \\ 0 \\ \frac{1+\mu_f\,\tan\theta}{m_2(\tan^2\theta+1)} \end{bmatrix}, \tag{12}$$

$$\mathbf{C}_1 = \begin{bmatrix} 0 & 1 & 0 & 0 \end{bmatrix}, \tag{13}$$

$$\mathbf{D}_{11} = 0. \tag{14}$$

In the presence of uncertainties, the nominal system is modified to introduce the variables corresponding to the uncertain parameters:

$$\dot{\mathbf{z}} = \mathbf{A}\mathbf{z} + \mathbf{B}_0\mathbf{u}_0 + \mathbf{B}_1\mathbf{u}_1,$$
$$\mathbf{y}_0 = \mathbf{C}_0\mathbf{z} + \mathbf{D}_{00}\mathbf{u}_0 + \mathbf{D}_{01}\mathbf{u}_1,$$
$$\mathbf{y}_1 = \mathbf{C}_1\mathbf{z} + \mathbf{D}_{10}\mathbf{u}_0 + \mathbf{D}_{11}\mathbf{u}_1. \tag{15}$$

In the case under consideration, the uncertainty is introduced on the friction coefficient μ_f. As there is only one uncertainty, the set $\mathbf{\Delta}_{\text{set}}$ is reduced to scalar variables, whose elements are noted δ. We have then $\tilde{\mu}_f = \mu_f(1 + \delta)$, where δ is the degree of uncertainty. The matrix $\mathbf{A}$ is then transformed to $\tilde{\mathbf{A}} = \mathbf{A} + \delta \cdot \bar{\mathbf{A}}$, where $\mathbf{A}$ is the previous matrix and $\bar{\mathbf{A}}$ is defined by

$$\bar{A} = \begin{bmatrix} 0 & 0 & 0 & 0 \\ 0 & 0 & 0 & 0 \\ 0 & 0 & 0 & 0 \\ -\frac{\mu_f k_1}{m_2(\tan^2\theta+1)} & \frac{\mu_f\,\tan\theta(k_1-k_2)}{m_2(\tan^2\theta+1)} & -\frac{\mu_f c_1}{m_2(\tan^2\theta+1)} & \frac{\mu_f\,\tan\theta(c_1-c_2)}{m_2(\tan^2\theta+1)} \end{bmatrix}. \tag{16}$$

By definition, we have $\mathbf{u}_0 = \delta \cdot \mathbf{y}_0$, which results in: $\delta \cdot \bar{\mathbf{A}} = \mathbf{B}_0 \cdot (\delta^{-1} - \mathbf{D}_{00})^{-1} \cdot \mathbf{C}_0$. This relation allows us to determine the matrices $\mathbf{B}_0$, $\mathbf{C}_0$ and $\mathbf{D}_{ij}$:

$$\mathbf{B}_0 = \begin{bmatrix} 0 \\ 0 \\ 0 \\ \frac{1}{m_2(\tan^2\theta+1)} \end{bmatrix}, \tag{17}$$

$$\mathbf{C}_0 = [-\mu_f k_1 \mu_f\,\tan\theta(k_1-k_2)-\mu_f c_1\,\mu_f\,\tan\theta(c_1-c_2)], \tag{18}$$

$$\mathbf{D}_{00} = 0, \tag{19}$$

$$\mathbf{D}_{01} = 0, \tag{20}$$

$$\mathbf{D}_{10} = 0. \tag{21}$$

The relations between $\mathbf{z}$, $\mathbf{y}_0$, $\mathbf{y}_1$, $\mathbf{u}_0$ and $\mathbf{u}_1$ determined in this section are the basis of the μ-synthesis resolution.

3.2.2. Resolution

As explained previously, Eqs. (16)–(21) correspond to the complete description of the controlled system and contain the nominal system and the perturbations linked to the uncertainties from a general standpoint.

The D–K iterations, allowing us to determine the robust controller by μ-synthesis, are conducted using Matlab software [28]. The controller is determined where the structured singular value μ of the system is less than unity and we obtain the Bode diagram of the controller allowing robust stability of the system.

The structured singular value μ obtained for the brake system is plotted in Fig. 4. We observe that μ is less than unity for all frequencies ω, which means that robust stability is assured. This result is obtained after two D–K iterations.

The controller determined by the algorithm and corresponding to this result is illustrated in Fig. 5. The controller is approximated by a function $G(\omega)$ which is sought in the form:

$$G(\omega) = -\alpha_G + \beta_G \omega^2, \tag{22}$$

where α_G and β_G are constants, depending on the values of the parameters of the system.

For the configuration $\omega_1 = 387 \, \mathrm{rad \, s^{-1}}$, $\omega_2 = 316.2 \, \mathrm{rad \, s^{-1}}$, $\zeta_1 = 0.008$, $\zeta_2 = 0.0065$ (i.e. $m_1 = 1 \, \mathrm{kg}$, $m_2 = 1 \, \mathrm{kg}$, $c_1 = 5 \, \mathrm{N \, m^{-1} \, s^{-1}}$, $c_2 = 5 \, \mathrm{N \, m^{-1} \, s^{-1}}$, $k_1 = 1.5 \times 10^5 \, \mathrm{N \, m^{-1}}$, $k_2 = 1 \times 10^5 \, \mathrm{N \, m^{-1}}$), $\theta = 0.2 \, \mathrm{rad}$, $\mu_f = 0.3$, the numerical results give $\alpha_G = 1 \times 10^5$ and $\beta_G = 0.9395$. This approximation of $G(\omega)$ allows a good representation of the controller, as we can see in Fig. 6, and it will be useful in the stability analysis of the controlled system.

3.3. Stability analysis of the initial and controlled systems

In this section, the stability of the initial and controlled brake systems will be compared. To examine the stability of the initial system, the eigenvalues λ of the matrix $\mathbf{A}$ (defined in Eq. (17)) need to be determined. As long as the real part of all the eigenvalues λ remains negative, the system is stable. When at least one of the eigenvalues has a positive real part, the system is unstable. Moreover, the imaginary part of the eigenvalue having a positive real part represents the frequency of the unstable mode.
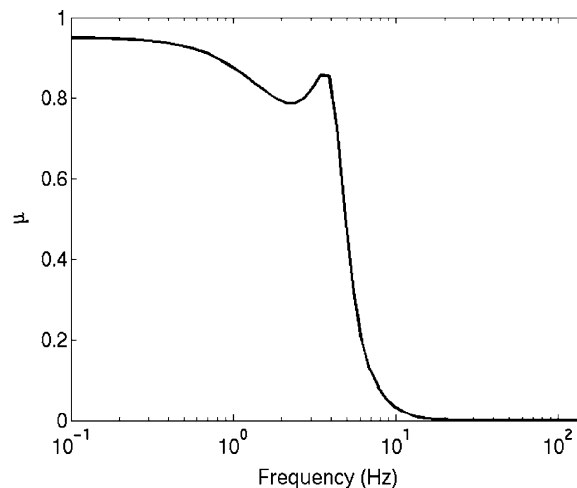
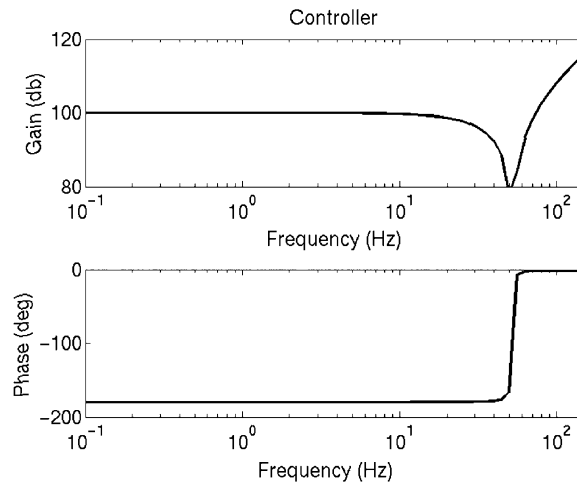

Fig. 4. Evolution of the structured singular value μ.
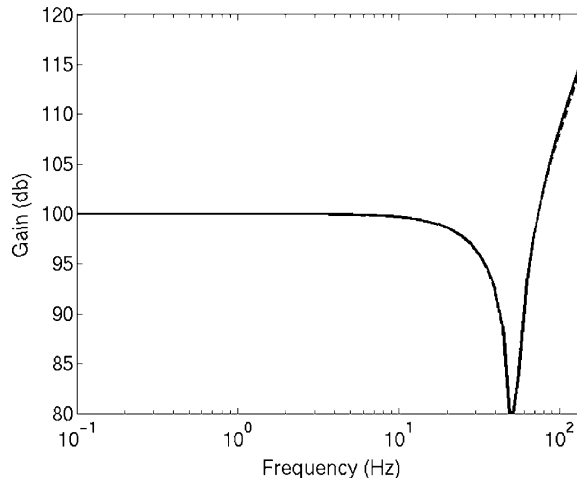
Fig. 5. Bode diagram of the controller.

Fig. 6. Approximation of the controller (------ result of the μ-synthesis, —— approximation).

For the controlled system, the form $G(\omega) = -\alpha_G + \beta_G \omega^2$ means that α_G is equivalent to a stiffness and β_G is equivalent to a mass. It enables us to take this into account directly in the mass and stiffness matrices. By noting $\tilde{\mathbf{K}}$ and $\tilde{\mathbf{M}}$ the new mass and stiffness matrices

$$\tilde{\mathbf{K}} = \mathbf{K} + \begin{bmatrix} 0 & 0 \\ 0 & 1 + \mu_f \tan \theta \cdot \alpha_G \end{bmatrix}, \tag{23}$$

$$\tilde{\mathbf{M}} = \mathbf{M} + \begin{bmatrix} 0 & 0 \\ 0 & 1 + \mu_f \tan \theta \cdot \beta_G \end{bmatrix}, \tag{24}$$

a new matrix $\tilde{\mathbf{A}}$ may be defined for the controlled system by

$$\tilde{\mathbf{A}} = -\begin{bmatrix} \mathbf{0} & \mathbf{I} \\ -\tilde{\mathbf{M}}^{-1}\tilde{\mathbf{K}} & -\tilde{\mathbf{M}}^{-1}\mathbf{C} \end{bmatrix}. \tag{25}$$

The advantage of these notations is that the stability analysis is similar for the initial and the controlled systems: the sign of the real part of the eigenvalues $\tilde{\lambda}$ of $\tilde{\mathbf{A}}$ gives the result concerning the stability of the system.

First, the evolutions of frequencies in relation to the brake friction coefficient for the initial and controlled brake systems are given in Fig. 7. The evolutions of the associated real parts and the representation in the complex plan are given in Figs. 8 and 9. As illustrated in Fig. 8, Hopf bifurcation points occur at $\mu_{f0} = 0.35$ and $\tilde{\mu}_{f0} = 0.46$ for the initial and controlled systems, respectively. A Hopf bifurcation point is defined by the following conditions:

$$\text{Re}(\lambda_{\text{center}}(\mu))|_{\mu_f = \mu_{f0}} = 0,$$

$$\text{Re}(\lambda_{\text{non-center}}(\mu))|_{\mu_f = \mu_{f0}} \neq 0,$$

$$\frac{\mathrm{d}}{\mathrm{d}\mu}(\boldsymbol{Re}(\lambda(\mu)))|_{\mu_f = \mu_{f0}} \neq 0, \tag{26}$$

where λ_{center} defines a pair of purely imaginary eigenvalues while all of the other eigenvalues $\lambda_{\text{non-center}}$ have non-zero real parts at $\mu_f = \mu_{f0}$. The last condition of Eq. (24), called a transversal condition, implies a transversal or non-zero speed crossing of the imaginary axis.
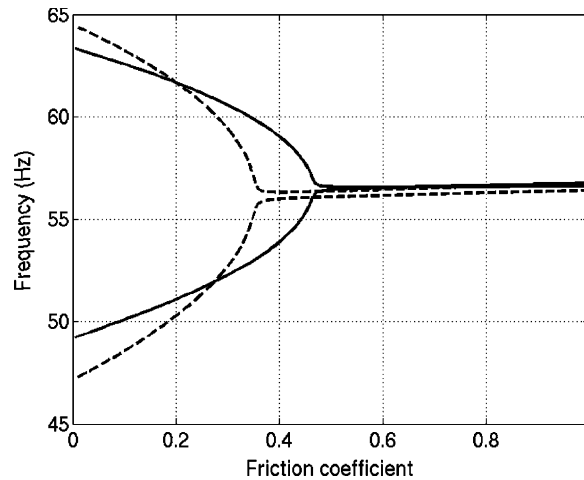

Fig. 7. Evolution of the frequency of two coupling modes (------ initial system, —— controlled system).
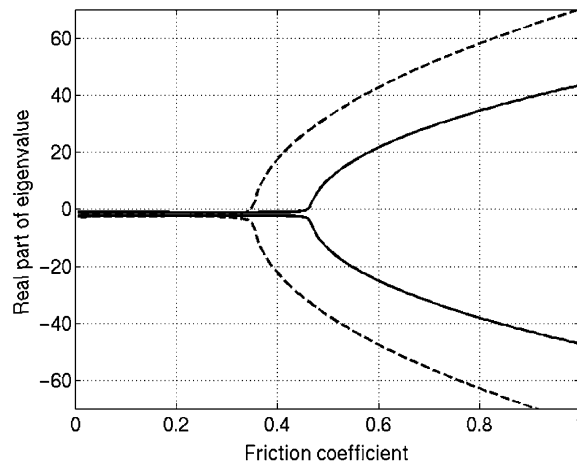

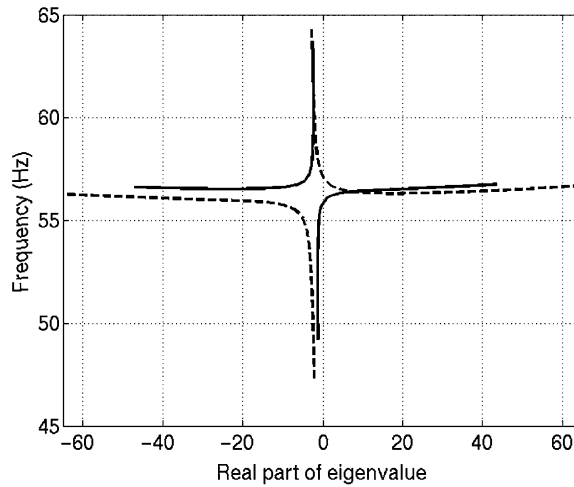Fig. 8. Evolution of the real part of two coupling modes (------ initial system, —— controlled system).

Fig. 9. Evolution of the frequency versus real part of two coupling modes (- - - - - - initial system, ——— controlled system).
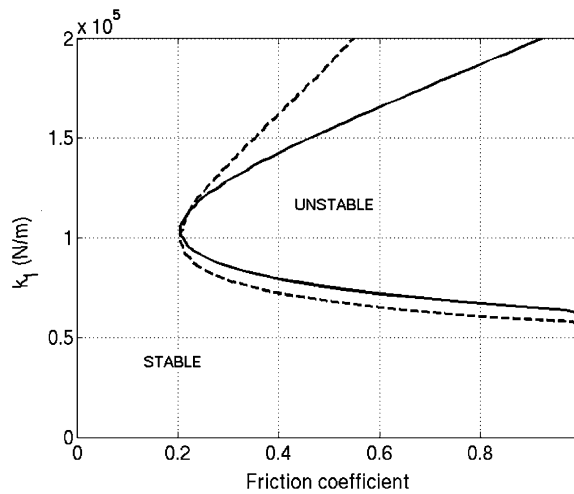

Fig. 10. Stability as a function of brake friction coefficient μ_f and stiffness k_1 (- - - - - - initial system, ——— controlled system).

If $\mu_f < \mu_{f0}$ the initial system is stable; it has two stable modes at different frequencies, as illustrated in Fig. 7. As the brake friction coefficient increases, these two modes move closer until they reach the bifurcation zone. We obtain the coalescence for $\mu_f = \mu_{f0}$ of two imaginary parts of the eigenvalues. Finally, the initial system becomes unstable for $\mu_f > \mu_{f0}$. In the case of the controlled brake system, the stable and unstable regions are obtained for $\mu_f < \tilde{\mu}_{f0}$ and $\mu_f > \tilde{\mu}_{f0}$, respectively.

In Fig. 8, it may be observed that the instability region versus the friction coefficient μ_f is smaller for the controlled system than for the initial system ($\tilde{\mu}_{f0} > \mu_{f0}$). This illustrates the suitability of robust control via μ-synthesis.

An interesting observation is that the mode that becomes unstable and reaches the bifurcation zone is different for the initial and controlled systems (Fig. 11).

Then, in order to demonstrate the suitability of μ-synthesis and in order to compare the stability analysis of the initial and controlled brake systems, different sets of two combinations of physical parameters k_1, k_2, c_1, c_2 and θ are tested. Figs. 10–14 show the zones of instability for the initial and controlled systems: the dashed line corresponds to the initial system and the solid line corresponds to the controlled system. Figs. 15 and 16 show the evolutions of the frequencies and the associated real parts in the complex plane.
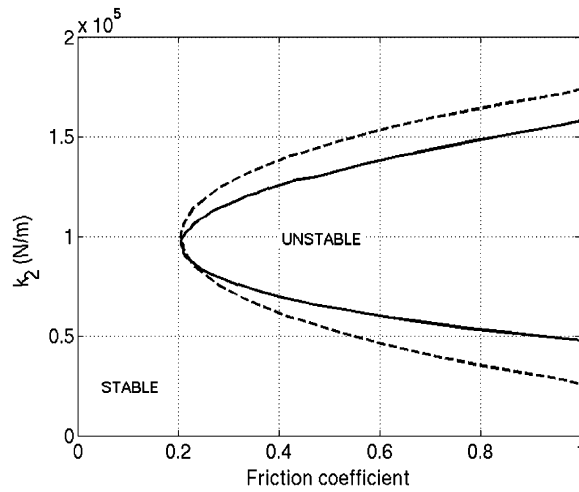
Fig. 11. Stability as a function of brake friction coefficient μ_f and stiffness k_2 (----- initial system, —— controlled system).
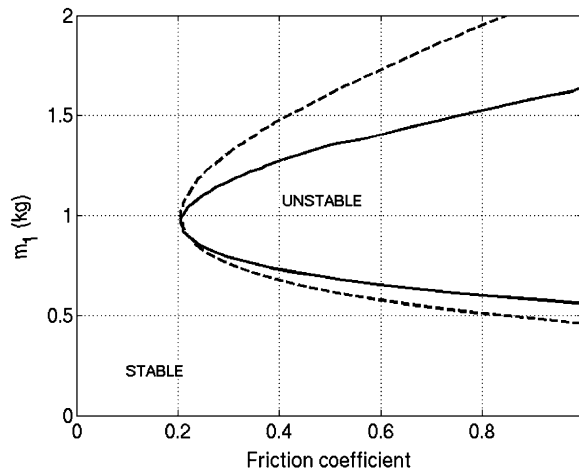

Fig. 12. Stability as a function of brake friction coefficient μ_f and mass m_1 (----------- initial system, —— controlled system).
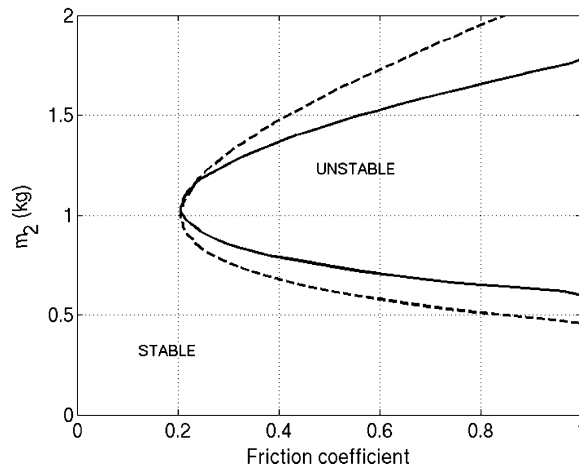

Fig. 13. Stability as a function of brake friction coefficient μ_f and mass m_2 (----- initial system, —— controlled system).
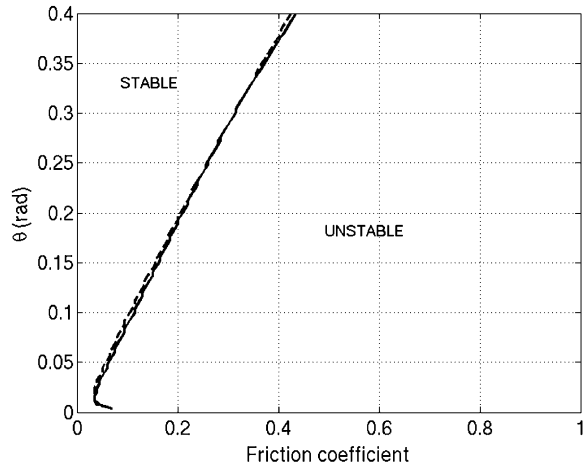
Fig. 14. Stability as a function of brake friction coefficient μ_f and angle θ (- - - - - initial system, —— controlled system).

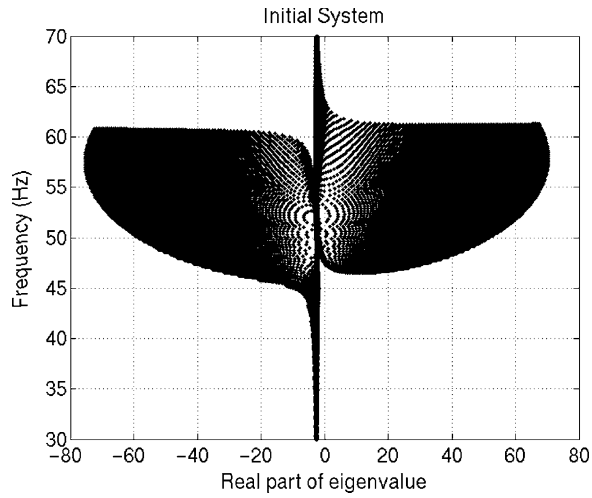

Fig. 15. Frequency and real part of eigenvalue of the initial system for various friction coefficients μ_f and stiffness k_1.
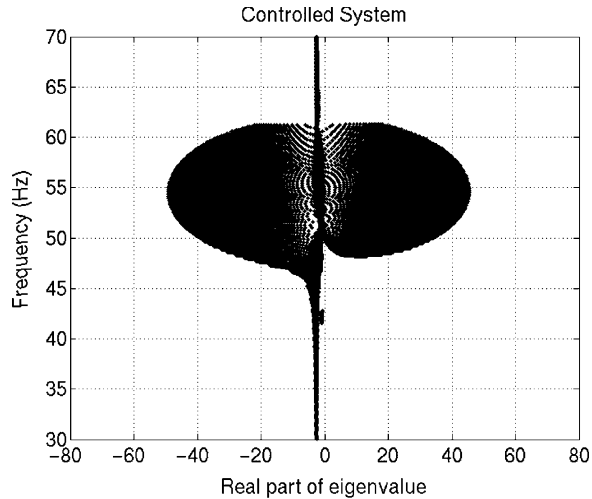

Fig. 16. Frequency and real part of eigenvalue of the controlled system for various friction coefficients μ_f and stiffness k_1.

For all tested combinations of the different parameters with the brake friction coefficient (Figs. 10–14), the controller provided by μ-synthesis allows an increased stable zone for the brake system. However, for some values of these parameters which correspond more or less to the nominal setting, this improvement is very weak. Another interesting result of μ-synthesis is that the intervals of instability frequencies are reduced for the controlled brake system in comparison with the initial system, as illustrated in Figs. 15 and 16 and Table 1.

Table 1
Comparison of the instability regions for the initial and controlled brake system

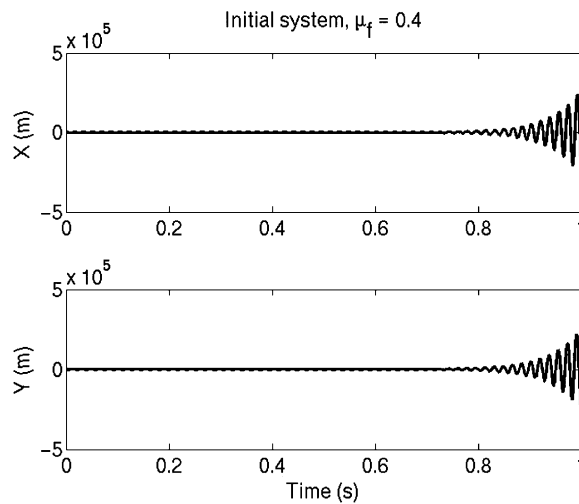| Parameter	Initial system (Hz)	Controlled system (Hz)
k_1	47–64	49–62
k_2	42–65	43–65
m_1	44–63	47–58
m_2	44–64	44–64
θ	51	49–52

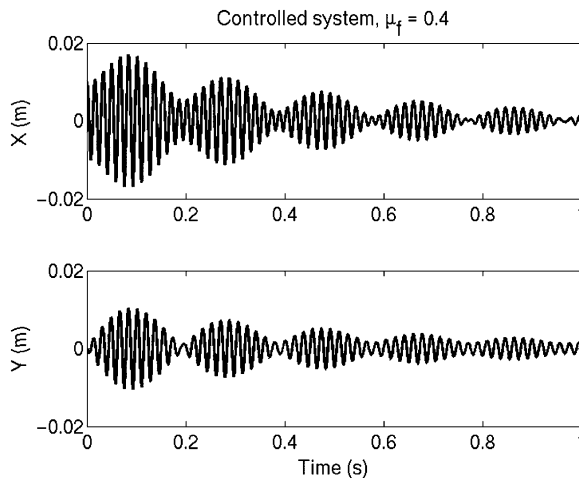Fig. 17. Temporal response of the initial system for $\mu_f = 0.4$.

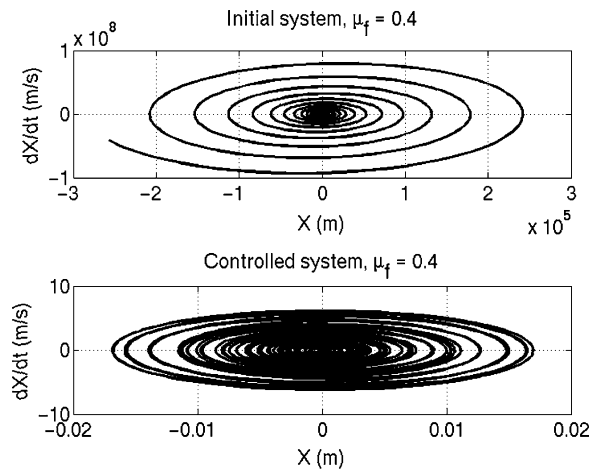Fig. 18. Temporal response of the controlled system for $\mu_f = 0.4$.

Fig. 19. Divergent oscillations for $\mu_f = 0.4 (\mu_{f0} < \mu_f < \tilde{\mu}_{f0})$.

Finally, dynamical responses of the system are presented in Figs. 17 and 18 in order to illustrate the advantages of the controlled brake system versus the initial brake system. In this case, we consider a combination of parameters corresponding to an unstable zone for the initial system and a stable zone for the controlled system ($m_1 = 1 \, \text{kg}$, $m_2 = 1 \, \text{kg}$, $c_1 = 5 \, \text{N m}^{-1} \, \text{s}^{-1}$, $c_2 = 5 \, \text{N m}^{-1} \, \text{s}^{-1}$, $k_1 = 1.5 \times 10^5 \, \text{N m}^{-1}$, $k_2 = 1 \times 10^5 \, \text{N m}^{-1}$, $\theta = 0.2 \, \text{rad}$, $\mu_f = 0.4$). In such a case, the temporal response of the initial system grows exponentially while that of the controlled system is softened (Figs. 17 and 18). Fig. 19 illustrates the oscillations of the initial and controlled systems. It illustrates the difference between the behaviour of the two systems. The instability is manifested by an exponentially increasing curve. On the other hand, the response of the controlled system is more complex but is limited in amplitude.

4. Conclusion

This study presents an application of μ-synthesis in order to eliminate friction-induced vibration for a brake system. A model for judder instability analysis and an associated stability analysis for the initial and controlled systems are developed. For further understanding of the effects caused by variations in some parameters and the suitability of μ-synthesis, a stability analysis using two parameter evolutions has been conducted.

Robust stability via μ-synthesis for brake systems appears interesting for reducing the size of the instability regions in relation to the possible system parameter combinations. This procedure can be applied to a brake design avoiding friction-induced judder instability.

References

[1] R.A. Ibrahim, Friction-induced vibration, chatter, squeal and chaos: Part I—mechanics of contact and friction, *ASME Applied Mechanics Review* 47 (7) (1994) 209–226.
[2] R.A. Ibrahim, Friction-induced vibration, chatter, squeal and chaos: Part II—dynamics and modeling, applied mechanics review, *ASME Applied Mechanics Review* 47 (7) (1994) 227–253.
[3] F.P. Bowden, D. Tabor, *The Friction and Lubrication of Solids*, second corrected ed, Oxford University Press, Clarendon Press, Oxford, 2001 (Oxford Classic Text in the Physical Sciences).
[4] E. Rabinowicz, *Friction and Wear of Materials*, Wiley, New York, 1965.
[5] B. Armstrong-Hélouvry, P. DuPont, C. Canudas de Wit, A survey of models, analysis tools and compensation methods for the control of machines with friction, *Automatica* 30 (7) (1994) 1093–1138.
[6] J.T. Oden, J.A.C. Martins, Models and computational methods for dynamic friction phenomena, *Computer Methods in Applied Mechanics and Engineering* 52 (1985) 527–634.
[7] M.R. North, 14th FISITA Congress, Paper 1/9, *A Mechanism of disc brake squeal*, 1972.
[8] M.R. North, ImechE, C38, *Disc brake squeal*, 1976.

 [9] D.A. Crolla, A.M. Lang, Tribologie, vehicle tribology, *Brake Noise and Vibration—State of Art* 18 (1991) 165–174.
[10] N.M. Kinkaid, O.M. O'Reilly, P. Papadopoulos, Automotive disc brake squeal, *Journal of Sound and Vibration* 267 (2003) 105–166.
[11] H. Ouyang, J.E. Mottershead, M.P. Cartmell, M.I. Friswell, Friction-induced parametric resonances in discs: effect of a negative friction velocity relationship, *Journal of Sound and Vibration* 2092 (1998) 251–264.
[12] H. Ouyang, J.E. Mottershead, D.J. Brookfields, S. James, M.P. Cartmell, A methodology for the determination of dynamic instabilities in a car disc brake, *International Journal of Vehicle Design* 23 (2000) 241–262.
[13] H. Ouyang, J.E. Mottershead, M.P. Cartmell, D.J. Brookfield, Friction-induced vibration of an elastic slider on a vibrating disc, *International Journal of Mechanical Sciences* 41 (3) (1999) 325–336.
[14] H. Ouyang, J.E. Mottershead, Unstable travelling waves in the friction-induced vibration of discs, *Journal of Sound and Vibration* 248 (4) (2001) 768–779.
[15] S.W.E. Earles, G.B. Soar, Squeal noise in disc brakes, in: *Proceedings of the Institution of Mechanical Engineers*, *Symposium on Vibration and Noise in Motor Vehicles*, Paper C100/71, 1971.
[16] S.W.E. Earles, M.N.M. Badi, SAE Paper 780331, *On the interaction of a two-pin-disc system with reference to the generation of disk-brake squeal*, 1978.
[17] N. Millner, SAE Paper 780332, *An Analysis of Disc Brake Squeal*, 1978.
[18] S.W.E. Earles, C.K. Lee. Trans ASME, Instabilities arising from the frictional interaction of a pin-disc system resulting in noise generation, *Journal of Engineering for Industry* 98 (Series B, no. 1) (1976) 81–86.
[19] H.R. Mills, 1938/1939 Research Report no. 9000B and Research Report no. 9162B of the Institution of Automobile Engineers, *Brake Squeal*, 1938/1939.
[20] S.W.E. Earles, P.W. Chambers, Disc brake squeal noise generation: predicting its dependency on system parameters including damping, *International Journal of Vehicle Design* 8 (4/5/6) (1987) 538–552.
[21] J.J. Sinou, F. Thouverez, L. Jezequel, Analysis of friction and instability by the centre manifold theory for a non-linear sprag-slip model, *Journal of Sound and Vibration* 265 (2003) 527–559.
[22] R.T. Spurr, A theory of brake squeal, *in: Proceedings of the Automotive Division, the Institution of Mechanical Engineers* 1 (1961) 33–40.
[23] R.P. Jarvis, B. Mills, Vibrations induced by dry friction, *in: Proceedings of the Institution of Mechanical Engineers* 178 (32) (1963/1964) 847–866.
[24] J.C. Doyle, Analysis of feedback systems with structured uncertainty, *IEE Proceedings, Part D* 129 (1982) 242–250.
[25] A. Packard, J. Doyle, The complex structured singular value, *Automatica* 29 (1) (1993) 71–109.
[26] A. Packard, J. Doyle, G.J. Balas, Linear, multivariable robust control with a μ perspective, *Journal of Dynamic Systems, Measurement and Control* 115 (1993) 426–438.
[27] P. Venini, Robust control of uncertain structures, *Computers & Structures* 67 (1998) 165–174.
[28] G.J. Balas, J. Doyle, K. Glover, A. Packard, R. Smith, μ-Analysis and Synthesis Toolbox (for use with MATLAB), The Math Works, Natick, MA, 1993.
[29] J. Markerink, S. Bennani, B. Mulder, *Design of a Robust Controller for the HIRM using μ-synthesis*, Report, GARTEUR (Group for Aeronautical Research and Technology in Europe), 1997.
[30] A. Lanzon, Pointwise in frequency performance weight optimization in μ-synthesis, *International Journal of Robust and Nonlinear Control* 15 (2005) 171–199.
[31] J.D. Wu, J.H. Lin, Implementation of an active vibration controller for gear-set shaft using μ-synthesis, *Journal of Sound and Vibration* 281 (2005) 1037–1055.
[32] J.P. Boudot, Modélisation des bruits de freinage des véhicules Industriels, Ph.D. Thesis, Ecole Centrale de Lyon, 1995.